

This article was downloaded by: [Siauliu University Library]

On: 17 February 2013, At: 06:59

Publisher: Taylor & Francis

Informa Ltd Registered in England and Wales Registered Number: 1072954 Registered office: Mortimer House, 37-41 Mortimer Street, London W1T 3JH, UK



Advanced Composite Materials

Publication details, including instructions for authors and subscription information:

<http://www.tandfonline.com/loi/tacm20>

Feasibility studies on active damage detection for CFRP aircraft bonding structures

Toshimichi Ogisu , Masakazu Shimanuki , Satoshi Kiyoshima , Yoji Okabe & Nobuo Takeda

Version of record first published: 02 Apr 2012.

To cite this article: Toshimichi Ogisu , Masakazu Shimanuki , Satoshi Kiyoshima , Yoji Okabe & Nobuo Takeda (2006): Feasibility studies on active damage detection for CFRP aircraft bonding structures, *Advanced Composite Materials*, 15:2, 153-173

To link to this article: <http://dx.doi.org/10.1163/156855106777873923>

PLEASE SCROLL DOWN FOR ARTICLE

Full terms and conditions of use: <http://www.tandfonline.com/page/terms-and-conditions>

This article may be used for research, teaching, and private study purposes. Any substantial or systematic reproduction, redistribution, reselling, loan, sub-licensing, systematic supply, or distribution in any form to anyone is expressly forbidden.

The publisher does not give any warranty express or implied or make any representation that the contents will be complete or accurate or up to date. The accuracy of any instructions, formulae, and drug doses should be independently verified with primary sources. The publisher shall not be liable for any loss, actions, claims, proceedings, demand, or costs or damages whatsoever or howsoever caused arising directly or indirectly in connection with or arising out of the use of this material.

Feasibility studies on active damage detection for CFRP aircraft bonding structures *

TOSHIMICHI OGISU ^{1,†}, MASAKAZU SHIMANUKI ¹,
SATOSHI KIYOSHIMA ¹, YOJI OKABE ² and NOBUO TAKEDA ²

¹ *Fuji Heavy Industries Limited, Aerospace Company, Engineering and Development Center, Research and Laboratory Department, Yonan 1-1-11, Utsunomiya, Tochigi, 320-8564, Japan*

² *Graduate School of Frontier Sciences, The University of Tokyo, Mail Box 302, 5-1-5 Kashiwanoha, Kashiwa, Chiba, 277-8561, Japan*

Received 29 October 2004; accepted 29 June 2005

Abstract—This paper presents a part of the feasibility study for employing a damage monitoring system using a PZT actuator/FBG sensor. The goal of this research is to improve the present safety level of aircrafts by ensuring structural integrity and reducing maintenance/operation costs of advanced composite materials that will be employed for the primary structures of the new generation aircraft. Our novel sensor system employing a PZT actuator and an FBG optical fiber sensor can detect several types of damage, such as delamination and debonding, which are expected to occur in the highly efficient bonding structures of an aircraft wing box when the main/tail wing section is designed using composite materials. In this system, elastic waves will be transmitted into the structure by PZT actuators and received by small-diameter FBG optical fiber sensors that are embedded in the critical section of the primary structure of an aircraft. The onset and growth of damage can be detected with a very high accuracy through the change in the received elastic waves.

In this study, a conceptual design was implemented in order to employ the novel system. We also selected the optimum application candidate area in order to verify the effects of the system. Further, the investigation and experiment on the novel sensor system that uses a bonded PZT actuator and an FBG sensor was carried out, and the basic damage detection technique was established based on the experimental results of the received elastic wave. Furthermore, compressive tests were carried out using the coupon specimen with an embedded small-diameter or standard-diameter optical fiber sensor. It was verified that the coupon specimen with an embedded small-diameter optical fiber suffered no degradation of its material properties.

Keywords: Damage monitoring system; piezo transducer (PZT) actuator/FBG sensor; aircraft structure; structural integrity; elastic wave; damage detection; structural health management.

*Edited by the JSCM.

[†]To whom correspondence should be addressed. E-mail: Ogisut@uae.subaru-fhi.co.jp

1. INTRODUCTION

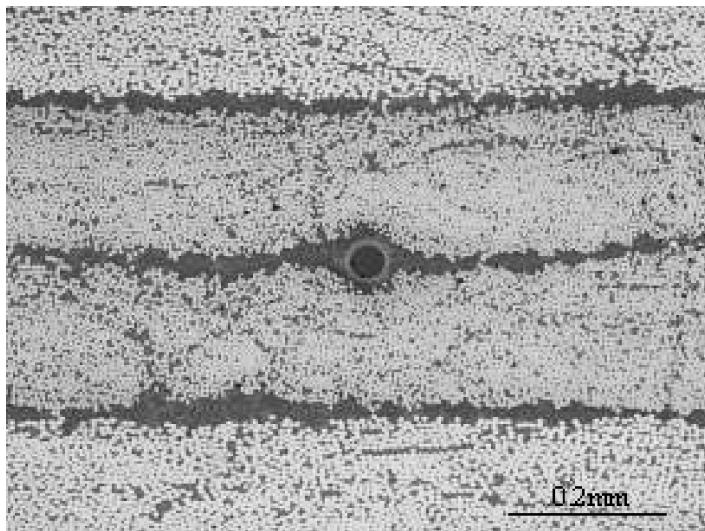
The application of composite materials in aircraft structures has increased in recent years, and this trend is expected to continue in the near future. Further, with an increase in the application of advanced composite materials, a corresponding increase in reliability and reduction in weight of the aircraft structures are essential [1]. In particular, the bonding structure is expected to play an important role in saving costs. However, these structures have many bonding lines that can be the weak points in the structure; these are referred to as 'hot spots' in the primary structure of the composite material.

The abovementioned problems should be resolved in order to increase the usage of composite materials. However, technologies that could enable detection of damage on bonding interfaces have not existed until now. Recently, novel technologies utilizing smart materials and structural systems have been developed. These systems can detect the onset and growth of damage in composite materials [2–5]. A PZT sensor system is expected to enable damage detection, and the feasibility studies for this system have progressed in co-operative research [6]. Many researchers have obtained similar results regarding the damage detection method for composite materials using an elastic (Lamb) wave launched from a PZT actuator [7, 8]. Moreover, the Comparative Vacuum Monitoring (CVM) technology using the extremely simple technique of measuring vacuum leakage is also becoming a topic of joint research for aircraft manufacturers [9]. The CVM is the most promising technique as a damage monitoring system for metallic material. These systems are extremely useful in detecting wide-range damage, but they do not possess sufficient accuracy to detect delamination and debonding in an adhesion interface of composite materials. Therefore, the authors are developing a novel sensor system using an FBG optical fiber, which is capable of detecting damage with a very high degree of accuracy [10].

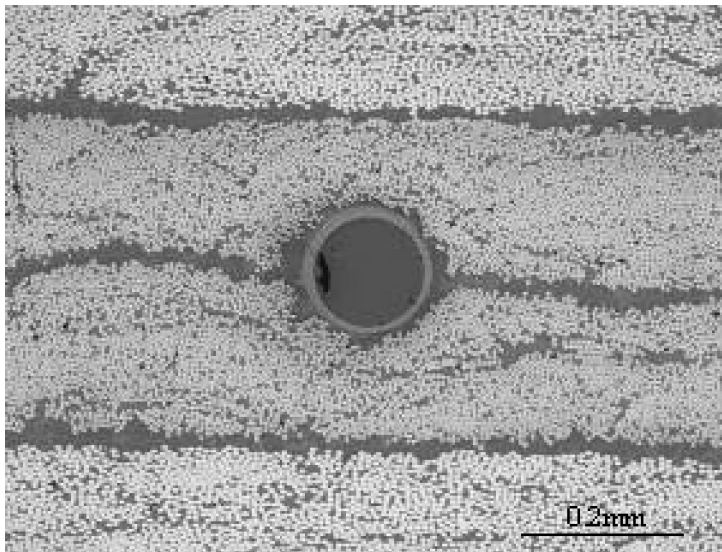
For example, when damage exists in the propagation path of an elastic wave, the damage information carried by the elastic wave is detected by a sensor. Here, since it is possible to embed the optical fiber near the damaged area, the FBG optical fiber sensor can detect the change in elastic wave propagation. Furthermore, the small-diameter optical fiber (outer diameter: 52 μm) [11] used in the present study (the standard diameter is 125 μm excluding its coating) can be embedded without degradation of the properties of the composite laminate. This is because it is significantly smaller than 125–200 μm in terms of the thickness of a lamina of general CF prepreg, and it can be embedded in an adhesive layer [12, 13]. Through the diagnosis of structural integrity using such a system, an increase in the reliability and reduction in weight of the advanced composite material can be expected. Figure 1 shows the cross-sectional view of the coupon specimen with embedded standard-diameter and small-diameter optical fibers in the CFRP laminate.

In this paper, the authors propose a novel hybrid damage monitoring system using a PZT actuator and an FBG optical fiber sensor. Additionally, a candidate

application area of the monitoring system is investigated. Further, the results of feasibility studies on both the elastic wave detection and the embedment effect of the optical fiber sensor are described.



(a)



(b)

Figure 1. Cross-section view of the CFRP laminate with an embedded optical fiber: (a) small-diameter and (b) standard-diameter.

2. STRUCTURAL HEALTH MONITORING IN AN AIRCRAFT STRUCTURE

Structural health monitoring has been recognized as a useful and necessary technology to promote the application of composite materials. The United States has already employed health-monitoring systems for composite liquid hydrogen tanks of reusable launch vehicles (RLV) and for aging aircrafts such as the B-52, C-130, F-15, etc. as a part of the maintenance program [14]. However, in general, design allowances for composite materials have been determined from the test data of the compression after impact (CAI) properties. Therefore, only approximately 25% of the characteristic compressive strength is used for the aircraft design [15]. One reason for this is that the onset and growth of the damage generated in a composite material cannot be easily detected using conventional NDI methods. Furthermore, sufficient weight reduction cannot be attained using conventional design techniques. Therefore, the CFRP laminate is referred to as ‘black aluminum’.

Consequently, the establishment of the constitutive equation (logical equation) and the damage monitoring system are required to ensure high reliability, low maintenance costs, and weight reduction. The damage monitoring technology is expected to satisfy these requirements. Therefore, aircraft manufacturers worldwide [8, 14] are also considering using this monitoring system for composite materials.

For example, if monitoring the onset and growth of damage in a composite material is possible by the deployment of the damage monitoring system, the reliability of composite materials will improve considerably. As shown in Fig. 2, establishing the prediction rule from the residual strength data of a coupon with

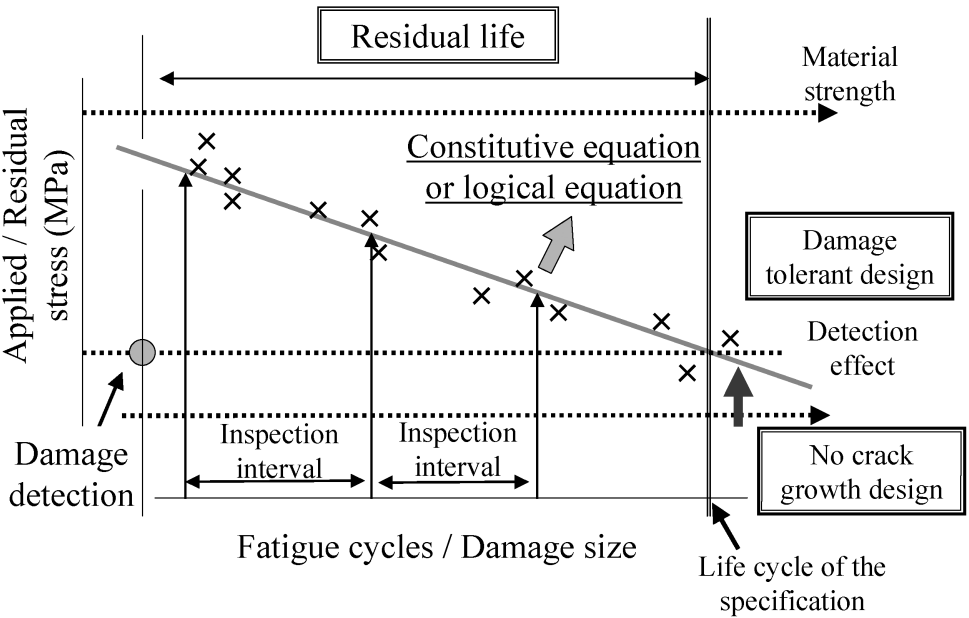


Figure 2. Effect of the SHM system in aircraft design.

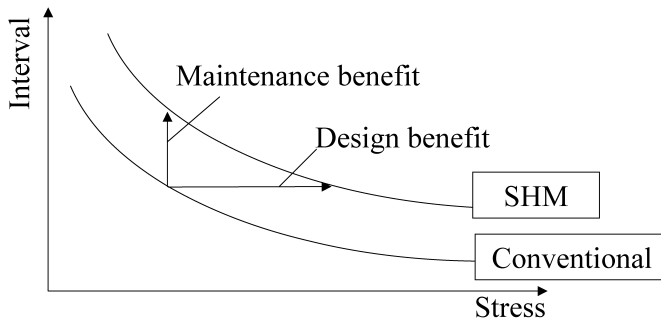


Figure 3. Benefit of structural health monitoring.

arbitrary damage sizes caused by the assumed flight cycle will be effective in reducing maintenance costs and weight. In Fig. 2, the symbol X indicates the relationship between the damage size and residual strength. The accumulation of these data will enable the construction of the constitutive equation. In the near future, the damage behavior analysis of composite materials will gain importance due to the improvement in the CAI properties. The change in design criteria from a no-damage-growth design to a damage-tolerance design is expected to be the next step in guaranteeing structural integrity through the accumulation of these data using damage monitoring technologies. Figure 3 shows the benefits of structural health monitoring for maintenance, cost reduction, and weight reduction [16].

3. PROPOSED STRUCTURAL HEALTH MONITORING SYSTEM

Figure 4 shows the basic device configuration of the damage monitoring system. The system proposed by the authors is a novel monitoring system that uses a piezoelectric element as an actuator (oscillating transmitter) and an FBG optical fiber as a sensor (receiver). If some damage exists in the traveling path of an elastic wave, the intensity of the wave will attenuate resulting in a change in the wave speed. Figure 5 is the schematic representation of the damage monitoring system applied to a wing box structure. In general, the conventional FBG sensor system can detect only dynamic strain with a frequency in the range of tens of kHz. Recently, there have been some new developments to measure dynamic strain ranging from 100 kHz to 1 MHz [17–19]. In our present study, we use a new FBG sensor system developed by Hitachi Cable Limited that can measure high-frequency waves with a high degree of accuracy [20]. An AWG-type filter is employed to obtain a characteristic high-sensitivity filter for detecting small displacements in the grating of FBG sensors. Figure 6 shows the concept of an AWG-type filter. In general, such AWG-type filters were used within the telecommunications field. This AWG filter has steep peaks, which are located at equal intervals of 0.8 nm. Therefore, we succeeded in developing a high-speed signal interrogating system by using the AWG-type filter.

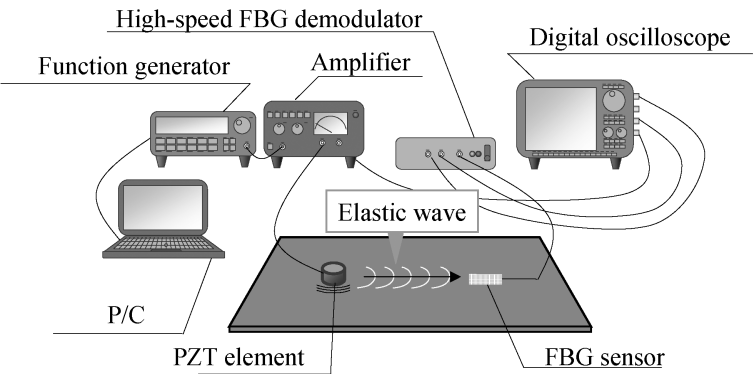


Figure 4. Set-up view of the damage monitoring system.

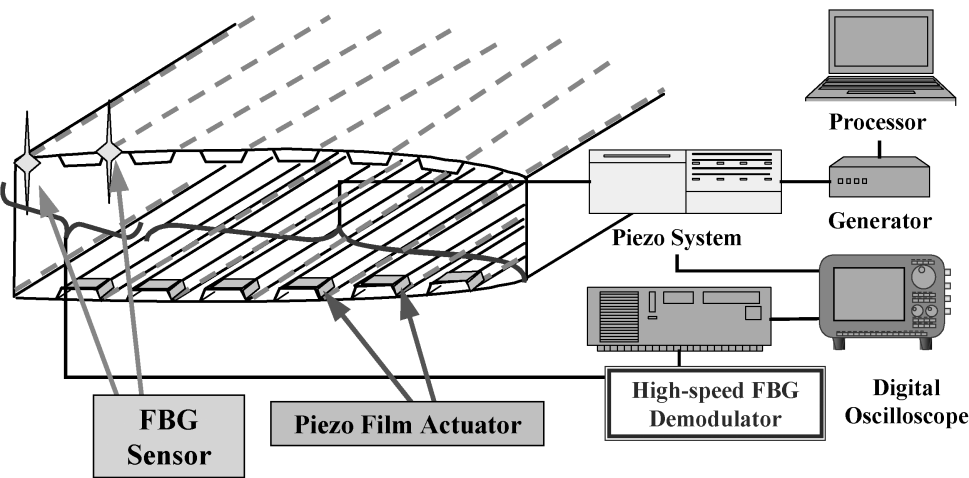


Figure 5. Damage monitoring system of a wing box structure.

Figure 7 shows the principle of Lamb wave detection using an AWG-type filter. Step 1 illustrates the generated image of the elastic (Lamb) wave in terms of the input voltages of the PZT element. Then, the elastic wave propagates to the host material as a microvibration of a strain. Step 2 illustrates the detected image of the elastic (Lamb) wave, which propagates through the structure. Here, when a vibration of the center wavelength of the FBG sensor occurs due to the microvibration of strain, the output signals of the AWG-type filters 1 and 2 increase and decrease in a cyclic manner by the oscillation of the wavelength of the FBG sensor. The output signal of the filter will then be obtained exactly as the signal of the reverse phase as shown in step 3. Thus, our monitoring system can detect the elastic wave.

These systems should be applied to a bonding structure as shown in Fig. 8. Since an internal defect such as delamination and debonding in the bonding structure is extremely difficult to detect, conventional NDI technology is inadequate for

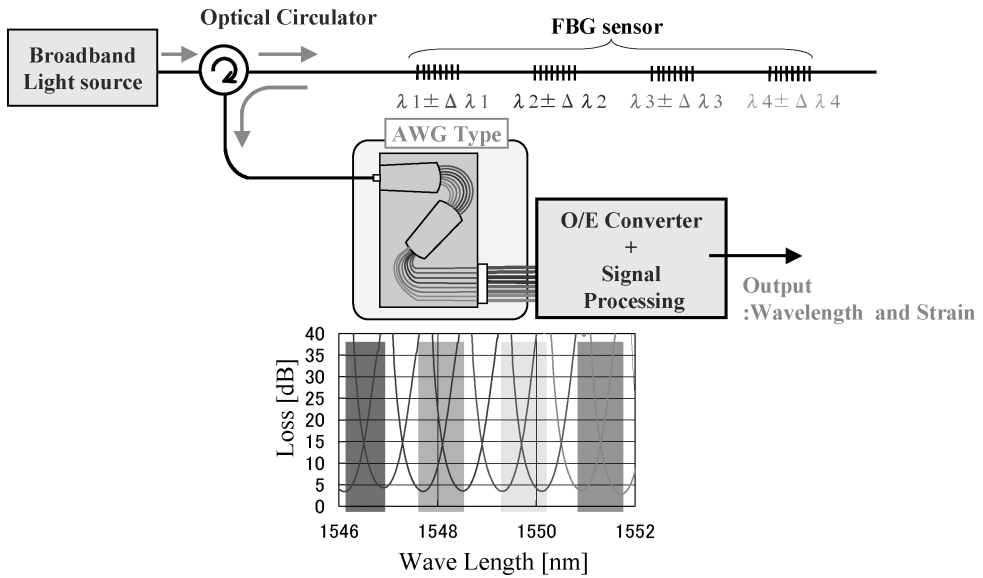


Figure 6. AWG-type filter of a FBG sensor.

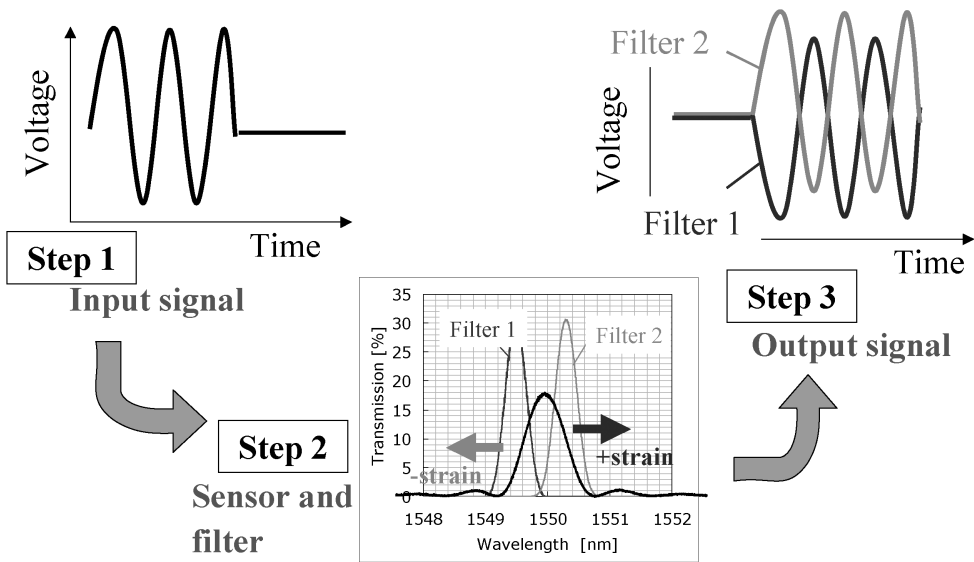


Figure 7. Principle of Lamb wave detection using an AWG-type filter.

this purpose. Moreover, such damage behavior of the structure has not been sufficiently investigated; further, high-accuracy damage detection using a novel damage monitoring system and accumulation of residual strength data depending on the damage size are required.

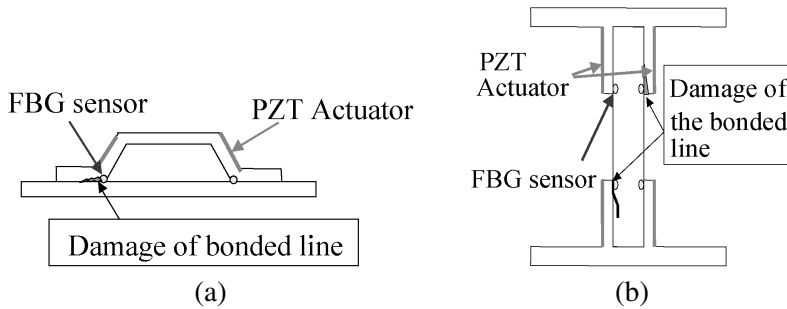


Figure 8. Schematic cross-section of (a) hat-shaped stringer and (b) π -shaped spar.

4. INVESTIGATION OF CANDIDATE APPLICATION AREA

The current design technique may not provide adequate safety and reliability for further weight reduction of composite materials. However, the application of SHM technologies such as damage monitoring systems presents the possibility of increasing the reliability and reducing the weight of composite materials. Therefore, the authors have considered the application of composite materials for the entire aircraft structure and investigated candidate application areas, as shown in Fig. 9. Considering the increase in the application of prospective composite materials, we should investigate the monitoring of all types of damage that occur in aircraft structures, which may become critical. However, in this study, we planned to verify the effectiveness of the damage monitoring system using a typical sub-component of the aircraft structure, which was decided based on the following evaluation criteria: (1) the utility to solve technical issues for the deployment of systems and (2) the technical verification of the one sub-component can be extended to complete aircraft structures.

Here, the monitoring of the target area was interpreted to be equivalent to that of the damage growth in the bonding interface of the skin/hat-shaped stringer, by taking into consideration aspects such as sensing technology to detect damage, system layouts (optical fiber arrangement, location, etc.), manufacturing issues (the embedment and drawing of the optical fiber, etc.) and the influence on material properties. Although the damage onset is expected to occur over the entire area, the authors selected the hat-shaped stringer/skin bonding structure as the candidate application area.

Figure 10 shows the hat-shaped stringer/skin interface as a typical critical area. In next-generation aircrafts, efficient adhesion structures are expected to be widely used with an increased application of composite materials. Therefore, the damage detection capability of the bonding lines will be a critical issue in the application of these composite materials. Consequently, the damage monitoring system of the bonding line proposed by the authors is expected to play an important role in aircraft safety.

In this case, the major advantage of the small-diameter optical fiber sensor is the visibility of the damage behavior of a bonding line in the composite materials,

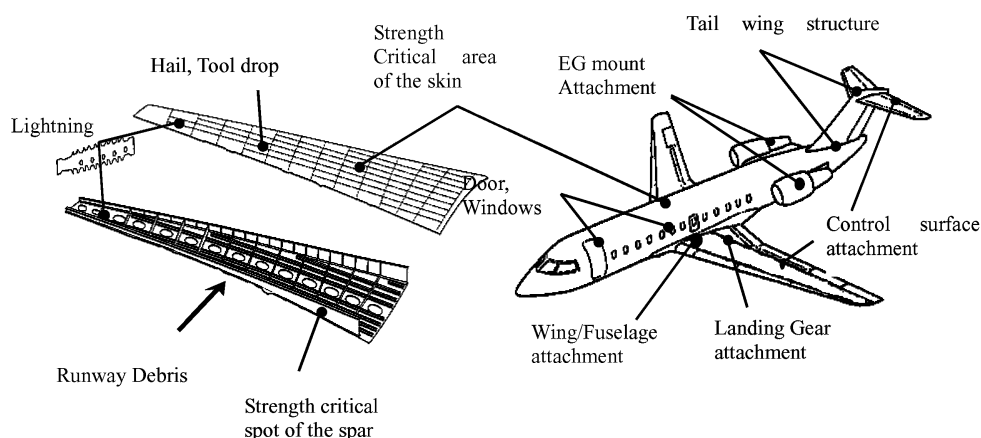


Figure 9. Application candidate area in the airframe.

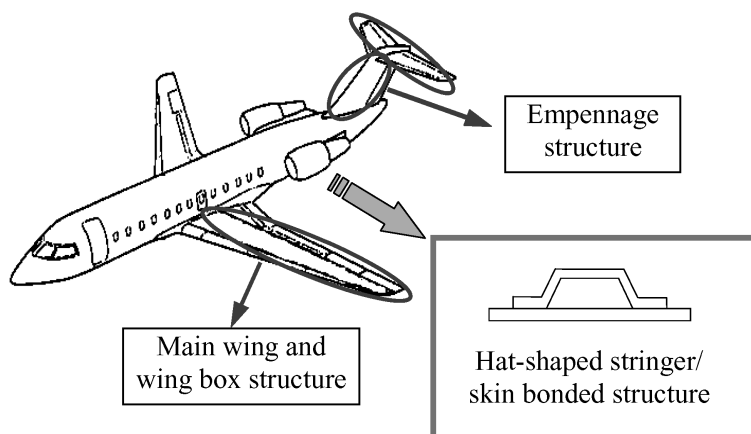


Figure 10. Hat-shaped stringer/skin bonded structure, as an investigated application area.

without the degradation of their material properties. The authors have assumed that the detection of the delamination and debonding of the hat-shaped stringer/skin interface, which cannot be achieved easily from the exterior, can be achieved by installing the small-diameter ($52\ \mu\text{m}$ in diameter) optical fiber sensor and a piezoelectric element actuator in the closed section of the bonding surface.

5. EXPERIMENTS

In order to assess the practicality of using the damage monitoring system described above, several types of experiments were conducted. The purpose of this research is the development of a damage monitoring system with embedded small-diameter FBG optical fiber sensors. However, we should acquire several sets of experimental data in order to investigate the basic susceptibility of the developed system.

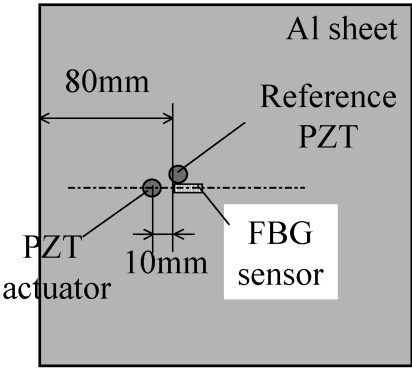


Figure 11. Set-up configuration for the elastic wave detection.

Therefore, in this paper, we describe the experimental data that are acquired using the bonded sensor system for practical application. Additionally, we estimate the material properties using a CFRP laminate with an embedded optical fiber sensor of either small or standard diameter.

5.1. Elastic wave detection technique

In the first experiment, the authors confirmed that the elastic wave with a center frequency of 300 kHz generated by the PZT actuator (Fuji Ceramics Corporation, Japan) could be detected using a standard-diameter FBG optical fiber sensor with a sensor length of 3 mm that was bonded on an aluminum sheet and an AWG-type filter. The input voltage of PZT was ± 75 V and the normalized treatment of the measurement data was conducted 256 times for noise removal. Figure 11 shows the setup configuration of the first experiment. Further, Fig. 12 shows the input signal to the PZT as well as the output signals from the PZT receiver and the FBG sensor. The output signals from the FBG sensor were plotted simultaneously for both filter 1 and filter 2. The shape of the output signal of the FBG sensor was in good agreement with that of the PZT receiver. Therefore, it was confirmed that an elastic wave with a center frequency of 300 kHz could be detected using the FBG sensor and the AWG-type filter.

5.2. Direction dependence of FBG sensors

We also evaluated the direction dependence of FBG sensors under the same condition as that of the first experiment. Figure 13 shows the setup configuration for the direction dependence test, while Fig. 14 shows the measurement results with respect to the direction dependence of the FBG sensor. The experiment was conducted at different propagation angles (0, 45, and 90 degrees) between the longitudinal direction of the FBG and the traveling path of the elastic wave. The test results confirmed that the wave amplitude decreased as the traveling path of an elastic wave shifted away from the axis of the FBG sensor. Therefore, it was verified

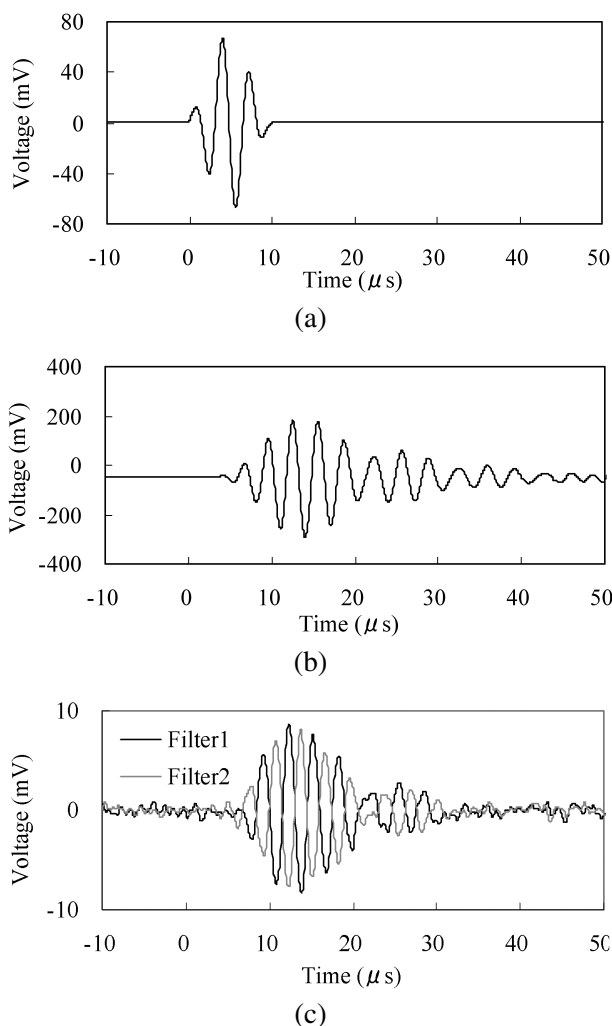


Figure 12. Results of the elastic wave detection using a FBG sensor: (a) Input signal, (b) Output signal of PZT element and (c) Output signal of FBG sensor.

that an FBG sensor exhibits strong direction dependence as compared with a PZT sensor.

5.3. Sensor length dependence of FBG sensors

Next, we confirmed that the elastic wave could be detected using a standard-diameter FBG optical fiber sensor of a certain sensor length, which was bonded on the CFRP cross-ply laminate (T700S/2500, $[0_2/90_2]_s$, thickness: 1 mm) and an AWG-type filter. The experimental conditions were the same as those in the first experiment. The authors also confirmed the dependence of the output signal behavior on the sensor length using sensor lengths of 1 mm, 3 mm, and 5 mm.

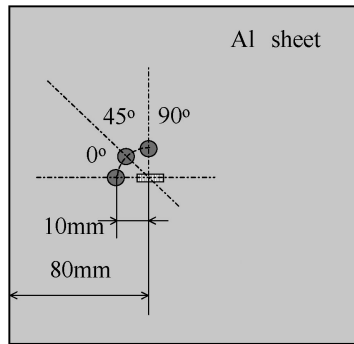
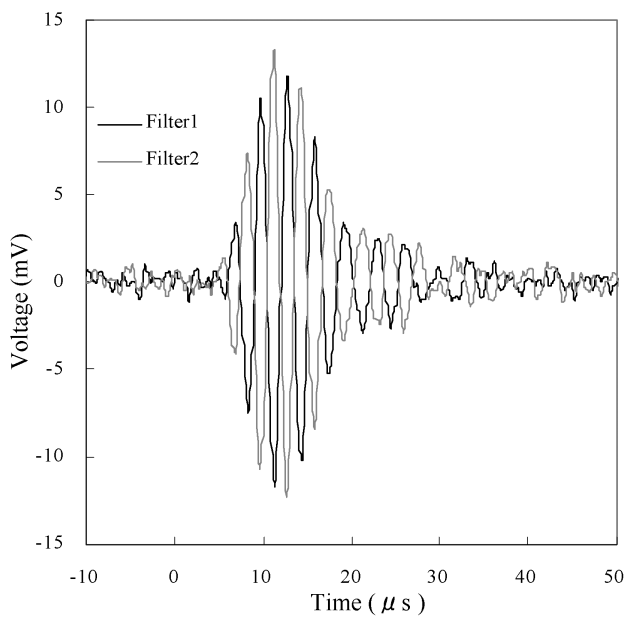


Figure 13. Set-up configuration for the direction dependence test.

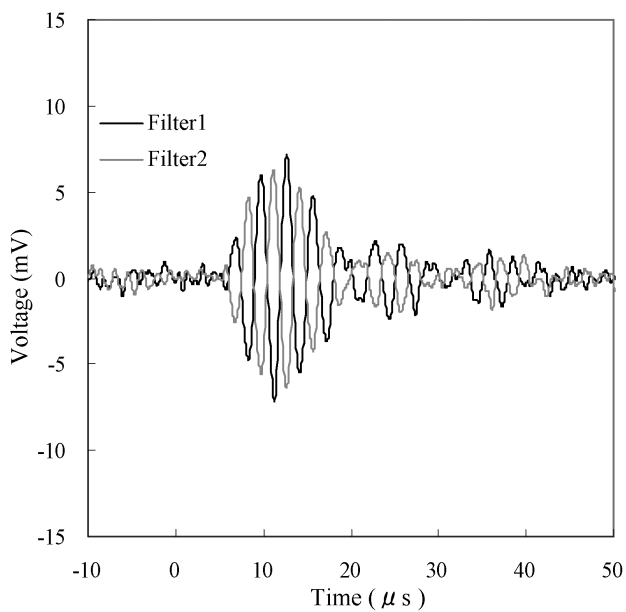
Figure 15 shows the setup configuration of the sensor length dependence test of the FBG sensor. Here, the distance between the PZT elements and FBG sensors is 30 mm. Figure 16 shows the output signal obtained from both the PZT actuators and FBG sensors, respectively. In general, the elastic wave at 300 kHz has two different wave modes — A_0 and S_0 . Therefore, the output signal of the PZT shows two wave modes in this experimental result. Similar to the output signal of the PZT, two different wave modes were also obtained from the output signal of the FBG sensors. In our monitoring system, if the elastic wave can be detected with high sensitivity, the output signal of the sensor shows the signal of the reverse phase. Therefore, with regard to the dependence of the sensor lengths, it was observed that the sensor sensitivity was inversely proportional to the sensor length. For example, the output signals of both filter 1 and filter 2 of a 1 mm gage length sensor can be obtained in the reverse phase with high resolution as compared with 3 mm and 5 mm gage length sensors. As a result, it is recognized that the FBG sensor can detect the elastic wave when the FBG sensor length is less than $1/7$ the wavelength of the elastic wave, as determined by theoretical analysis [12]. The results of the analysis also demonstrated that the elastic wavelength with a center frequency of 300 kHz was calculated to be 7 mm in the A_0 mode and 20 mm in the S_0 mode. Therefore, in the case of a 1 mm gage length, which is $1/7$ of the wavelength in the A_0 mode, it was confirmed that the elastic wave including both the A_0 and S_0 modes could be detected with good sensitivity.

5.4. Establishment of a basic damage detection technique

Based on the aforementioned result, the detection of delamination, which exists in a CFRP cross-ply laminate, was attempted. Delaminated coupon test specimens were manufactured by stripping off the Teflon film embedded in the 0/90 layers of the CFRP cross-ply laminate in order to obtain artificial delamination. The elastic wave generated by the PZT actuator was propagated through the delamination. On the other hand, a simulation of the output signal was performed under the same



(a)



(b)

Figure 14. Direction dependence of FBG sensor output: (a) $\theta = 0^\circ$, (b) $\theta = 45^\circ$ and (c) $\theta = 90^\circ$.

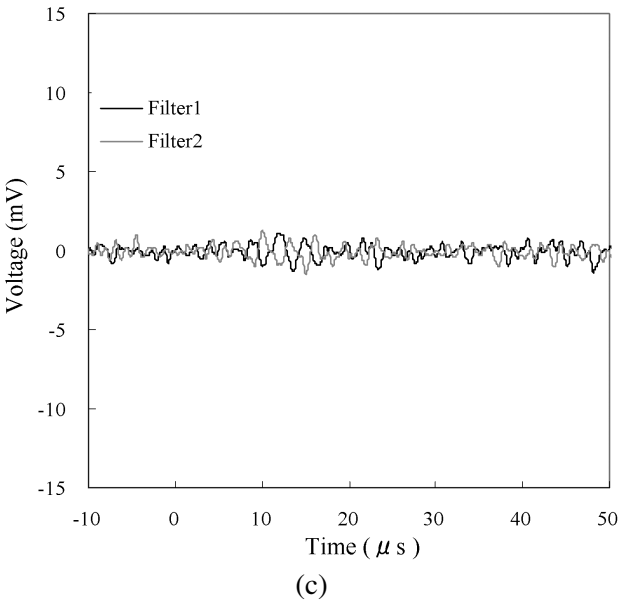


Figure 14. (Continued).

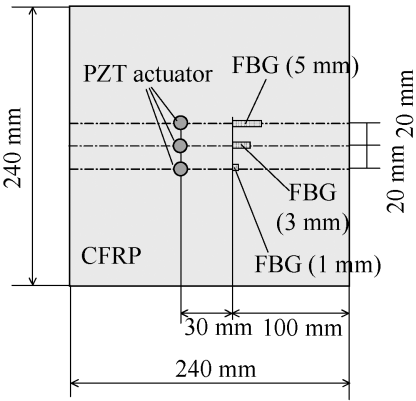


Figure 15. Set-up configuration of FBG sensor length dependence test.

conditions as the experiment in two cases, with and without delamination, using the wave analysis software ‘PZFLEX’ in order to undertake a theoretical consideration.

Figure 17 shows the setup configuration for the establishment of the damage detection technique, while Fig. 18 shows the experimental results. The ‘Experiment’ shown in Fig. 18 represents the output waveform of the FBG sensor with and without delamination and the output waveform of the PZT receiver with delamination. On the other hand, ‘Simulation’ represents the results of the simulation by theoretical analysis. This experiment confirmed that the new mode waveform appeared between the A_0 and S_0 modes when delamination existed throughout the laminate. This phenomenon occurred due to the separation of the A_0 mode, which was gen-

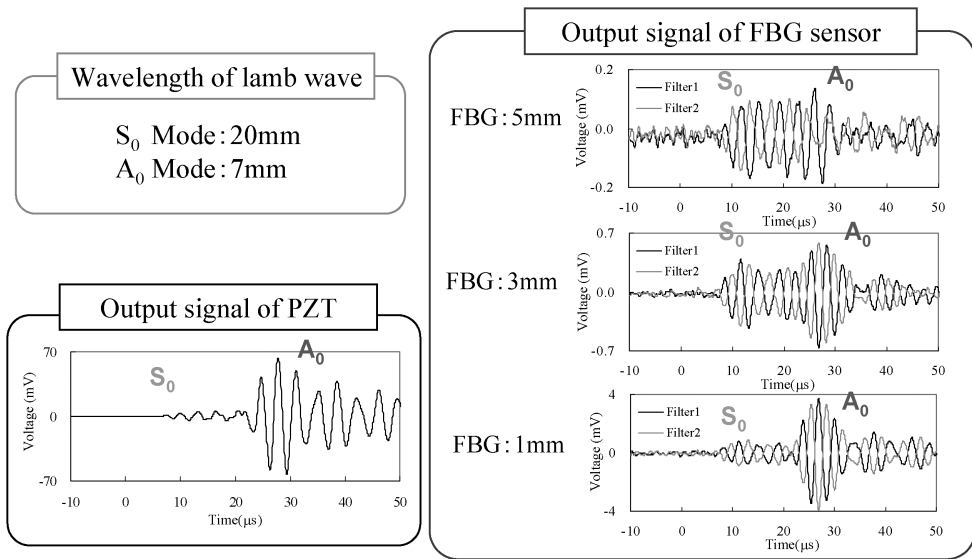


Figure 16. Dependence on the sensor length of FBG optical fiber sensor.

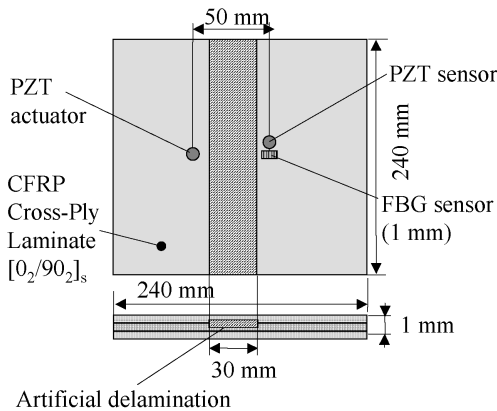


Figure 17. Set-up configuration for establishment of damage detection technique.

erated by the change in wave speed between $[0_2]$, the uppermost layers of delamination, and $[90_4/0_2]$, the lowermost layer of the delamination. The change in the received waveform presents the possibility of detection of delamination.

5.5. Influence of embedded optical fiber on material properties

5.5.1. Material. In this study, the CF prepreg system, T800/3900 series (TORAY) was used. Small-diameter (Hitachi Cable Ltd.) and standard-diameter optical fibers were embedded in CFRP laminates. In order to investigate the influence of the embedment of the optical fiber on the material properties, compressive tests were carried out using the coupon specimen, as shown in Fig. 19.

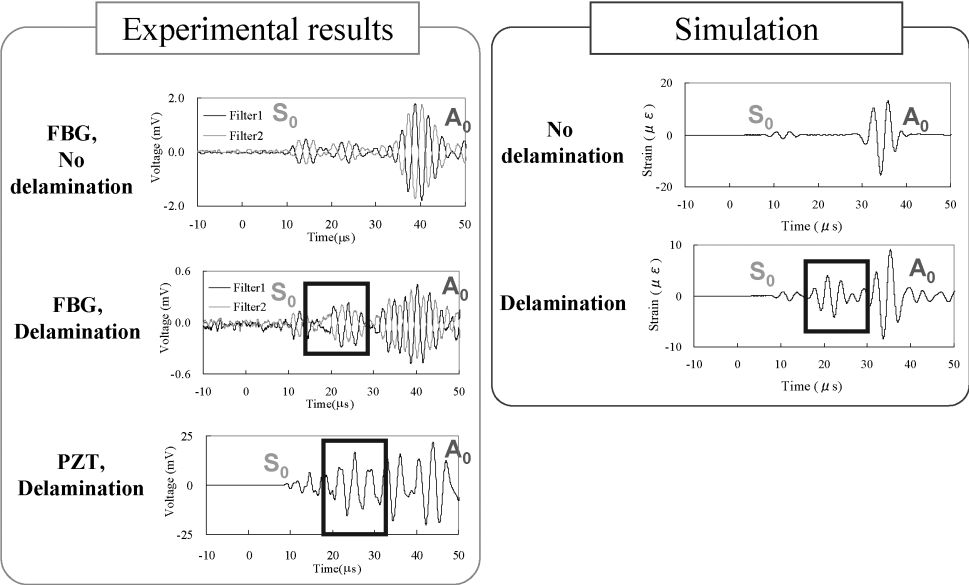


Figure 18. Damage detection of the cross-ply laminate using an FBG sensor.

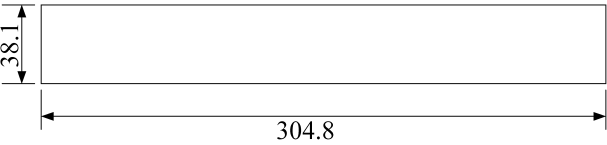


Figure 19. Configuration of an NHC-type specimen.

5.5.2. Specification of test coupon. The coupon used for the experiment is a flat panel with a basic stacking sequence $([45/0/-45/90]_{2S}, 16 \text{ ply})$. In order to simulate the manufacturing technique of the structure with the optical fiber embedded at the hat-shaped stringer/skin interface, the authors applied the co-bonding process, which cured the lay-up of ply No. 10 (optical fiber), ply No. 9 (adhesion film), and plies No. 1–8 (after curing the laminate of plies No. 11–18), as shown in Table 1. The optical fiber was arranged at two locations — 0 and 90 degrees of the carbon fiber (designated by L and T specimens, respectively) in parallel direction — at intervals of 12.5 mm (1/2 inch), as shown in Fig. 20. Here, the prepared optical fibers are of two types, i.e. small and standard diameters. The coupon specimen is cut out from these panels as an NHC-type specimen, as shown in Fig. 19.

5.5.3. Experimental procedure. Figure 21 shows the setup view of an NHC-type test. This test was conducted in accordance with SACMA SRM 3R-94 at room temperature after the testing machine (Instron Model 4482) was set up. The applied strain of the coupon specimens was measured at their centers using strain gages

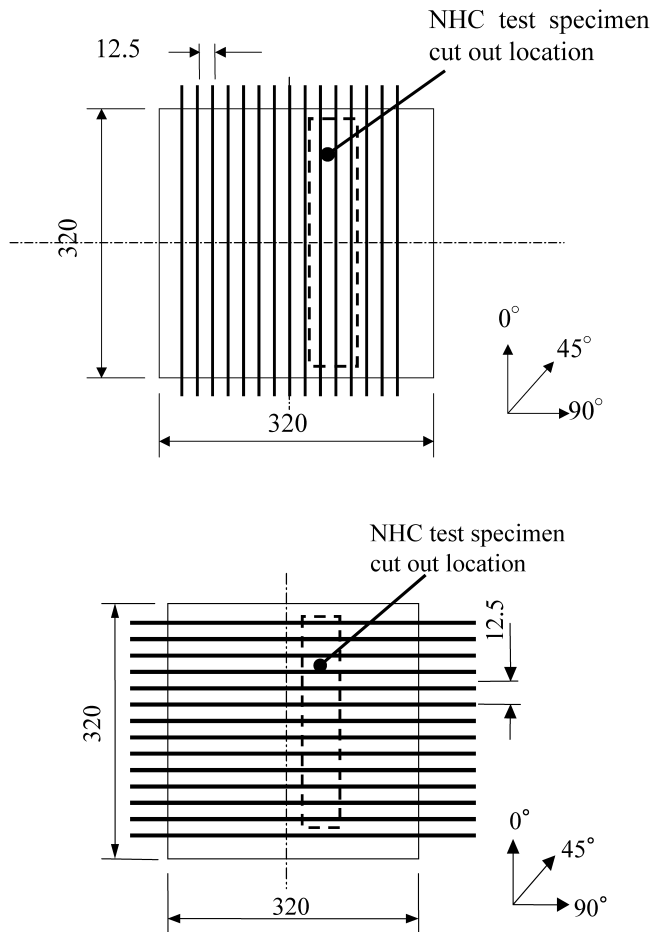


Figure 20. Test panel of coupon specimen.

(Tokyo Sokki Ltd., FCU-6-5-1L) attached on both sides using a dynamic strain measurement device (Tokyo Sokki Ltd. DRA-101A) in real time.

5.5.4. Experimental results. Figure 22 shows the results of the compressive test conducted on coupon specimens with either small-diameter ($52\ \mu\text{m}$ in diameter) or standard-diameter ($125\ \mu\text{m}$ in diameter) optical fibers and without an optical fiber. Error bars indicate both the minimum and maximum values in 99% fracture probability at 95% confidence. As observed from the results, it was confirmed that the strength data of the coupon specimen with an embedded standard-diameter optical fiber decreased by approximately 30 MPa for both the L and T specimens. On the other hand, the compressive strength of the coupon specimen with a small-diameter optical fiber remained unchanged as compared with CFRP laminate alone.

Table 1.
Stacking sequence of the test specimen

Ply No.	Material	Fiber orientation	Splice control
1	T800/3900 Type	45°	Butt splice ↑ ↓
2	T800/3900 Type	0°	
3	T800/3900 Type	−45°	
4	T800/3900 Type	90°	
5	T800/3900 Type	90°	
6	T800/3900 Type	−45°	
7	T800/3900 Type	0°	Butt splice
8	T800/3900 Type	45°	
9	Adhesive film	—	—
10	Optical fiber	—	—
11	T800/3900 Type	45°	Butt splice ↑ ↓
12	T800/3900 Type	0°	
13	T800/3900 Type	−45°	
14	T800/3900 Type	90°	
15	T800/3900 Type	90°	
16	T800/3900 Type	−45°	
17	T800/3900 Type	0°	
18	T800/3900 Type	45°	

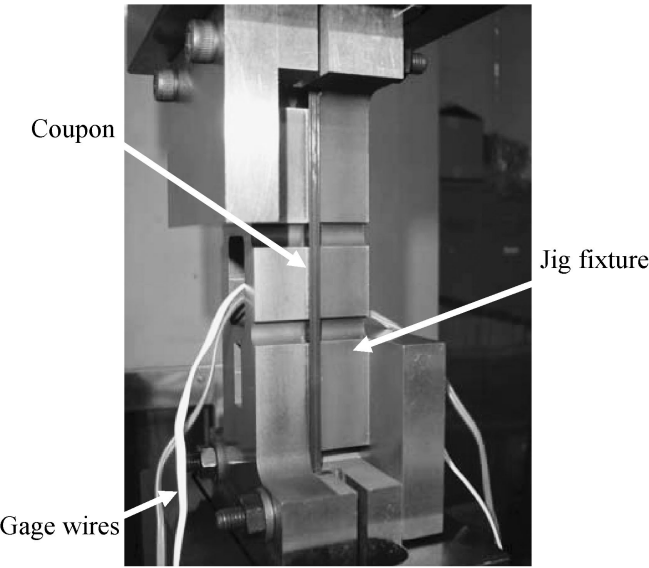


Figure 21. Set-up view of an NHC (No hole compression) test.

From the above result, it was verified that there was no degradation of the material properties of the CFRP composite laminate with an embedded small-diameter optical fiber.

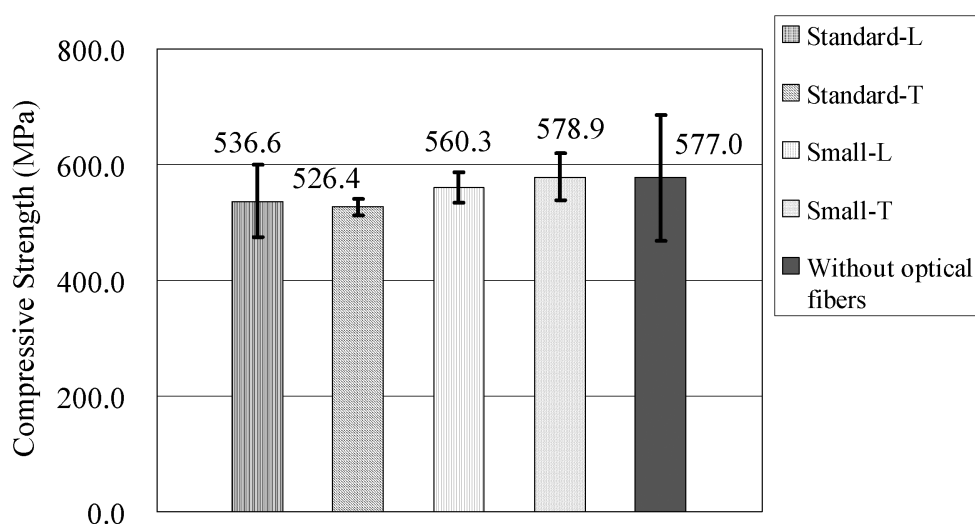


Figure 22. Influence of embedded small-diameter and standard-diameter optical fiber on composite strength at room temperature. Optical fibers are embedded parallel (L) or normal (T) to 0 degree direction.

6. CONCLUSIONS

The following results were obtained through the present research:

- (1) An active sensing system that can detect the onset and growth of damage in composite materials by using an FBG optical fiber sensor that receives elastic waves was proposed.
- (2) The conceptual design of a small passenger commercial jet constructed entirely from composite materials was investigated, and the assumed areas for the onset and growth of damage in the airframe were considered in order to test the active sensor system. Further, candidate application areas for the damage monitoring system were proposed.
- (3) The elastic wave detection test was conducted using the novel monitoring system, and it was verified that the elastic wave acquisition for a frequency of 300 kHz within a distance of 5 cm is possible by using an FBG optical fiber sensor bonded on an aluminum sheet and a CFRP cross-ply laminate.
- (4) The basic damage detection technique was established for the cross-ply CFRP laminate with delamination using the novel sensing system.
- (5) It was verified that a CFRP laminate with an embedded small-diameter optical fiber showed no degradation in the compressive strength.

Acknowledgement

This study was conducted as a part of the project, 'Civil Aviation Fundamental Technology Program-Advanced Materials and Process Development for Next-Generation Aircraft Structures' under contract from NEDO (New Energy and

Industrial Technology Development Organization) founded by the METI (Ministry of Economy, Trade and Industry), Japan.

REFERENCES

1. H. J. Schmidt and B. Schmidt-Brandecker, Structure design and maintenance benefits from health monitoring systems, in: *Proc. 3rd International Workshop on Structural Health Monitoring: The Demands and Challenges*, pp. 80–101 (2001).
2. M. Lin, Development of SMART layer for built-in structural diagnostics, in: *Proc. 2nd International Workshop on Structural Health Monitoring*, pp. 612–621 (1999).
3. Y. Okabe, T. Mizutani, S. Yashiro and N. Takeda, Application of small-diameter FBG sensors for detection of damage in CFRP composite, in: *Proc. 8th SPIE Smart Structures and Materials 2001*, Vol. 4328, pp. 295–305 (2003).
4. J. M. Menendez, P. Munoz, J. M. Pintado and A. Guemes, Damage detection in composite materials by FBGs, in: *Proc. 2nd European Workshop on Optical Fiber Sensors*, Vol. 5502, pp. 451–454 (2004).
5. T. Ogisu, M. Shimanuki, S. Kiyoshima, J. Takaki, I. Taketa and N. Takeda, Damage suppression system using embedded SMA foil in CFRP laminate structure, in: *Proc. 10th SPIE Smart Structures and Materials 2003*, Vol. 5054, pp. 192–202 (2003).
6. M. Lin, A. Kumar, X. Qing, S. J. Beard, S. S. Russell, J. L. Walker and T. K. Delay, Monitoring the integrity of filament wound composite pressure vessels using built-in sensor networks, in: *Proc. 10th SPIE Smart Structures and Materials 2003*, Vol. 5054, pp. 222–229 (2003).
7. C. Bollor, J. B. Ihn, W. J. Staszewski and H. Speckmann, Design principles and inspection techniques for long life endurance of aircraft structure, in: *Proc. 3rd International Workshop on Structural Health Monitoring: The Demands and Challenges*, pp. 275–283 (2001).
8. B. Beral and H. Speckmann, Structural health monitoring (SHM) for aircraft structures: A challenge for system developers and aircraft manufacturers, in: *Proc. 4th International Workshop on Structural Health Monitoring 2003*, pp. 12–29 (2003).
9. H. Stehmeier and H. Speckmann, Comparative vacuum monitoring (CVM): Monitoring of fatigue cracking in aircraft structure, in: *Proc. 2nd European Workshop on Structural Health Monitoring 2004*, pp. 367–373 (2004).
10. T. Ogisu, M. Shimanuki, S. Kiyoshima, Y. Okabe and N. Takeda, Development of damage monitoring system for aircraft structure using a PZT actuator/ FBG sensor hybrid, in: *Proc. 11th SPIE Smart Structures and Materials 2004*, Vol. 5388, pp. 425–436 (2004).
11. K. Satori, Y. Ikeda, Y. Kurosawa and A. Hongo, Development of small-diameter optical fiber sensors for damage detection in composite laminates, in: *Proc. Smart Materials Symposium*, pp. 91–94 (1999).
12. Y. Okabe and Takeda, *et al.*, Damage identification in composite laminates using small-diameter fiber Bragg grating sensors, in: *Proc. 3rd International Workshop on Structural Health Monitoring: The Demands and Challenges*, pp. 1165–1173 (2001).
13. H. Hanselka, Overview of German industrial research project ADAPTRONIK, in: *Proc. 7th SPIE Smart Structures and Materials 2000*, Vol. 3991, pp. 2–10 (2002).
14. P. Goggin, J. Huang, E. White and E. Haugse, Challenges for SHM transition to future aerospace systems, in: *Proc. 4th International Workshop on Structural Health Monitoring 2003*, pp. 30–41 (2003).
15. M. Chun-Yung Niu, *Composite Airframe Structures, Practical Design Information and Data*. Connilt Press Limited (1992).
16. C. D. Donne, National Review of Germany, ICAF2003, Switzerland (2003).
17. I. Perez, H. L. Cui and E. Udd, Acoustic emission detection using fiber Bragg gratings, in: *Proc. 8th SPIE Smart Structures and Materials 2000*, Vol. 4328, pp. 209–215 (2001).

18. C. S. Baldwin and A. J. Vizzini, Acoustic emission crack detection with FBG, in: *Proc. 10th SPIE Smart Structures and Materials 2003*, Vol. 5050, pp. 133–143 (2003).
19. D. C. Betz, G. Thursby, B. Culshaw and W. J. Staszewski, Lamb wave detection and source location using fiber Bragg grating rosettes, in: *Proc. 10th SPIE Smart Structures and Materials 2003*, Vol. 5050, pp. 117–126 (2003).
20. S. Kojima, A. Hongo, S. Komastuzaki and N. Takeda, High speed optical wavelength interrogator using a PLC-type optical fiber for fiber Bragg grating sensors, in: *Proc. 11th SPIE Smart Structures and Materials 2004*, Vol. 5384, pp. 241–249 (2004).